Int. J. Electrochem. Sci., 11 **(2016)** 2408 - 2418

International Journal of
ELECTROCHEMICAL
SCIENCE
www.electrochemsci.org

Short Communication

Synthesis of Yttrium Doped TiO_2 Nanotubes by a Microwave Refluxing Method and Their Photoluminescence Properties and Photocatalytic Properties

Jinsong Rao, Hansong Xue[*]*, Weina Zhang, Xinyu Li, Xiaochang You, Zhihui Xing*

College of Materials Science and Engineering, Chongqing University, Chongqing, 400044, China
[*]E-mail: hsxue@sohu.com

Received: 1 November 2015 / *Accepted:* 17 December 2015 / *Published:* 1 February 2016

Pure and Y-doped titanium dioxide (TiO_2) nanopowders were synthesized by sol-gel methed. The corresponding TiO_2 nanotubes were successfully synthesized by a microwave refluxing method using the as-prepared nanopowders as precursor subsequently. TiO_2 nanotubes and nanopowders were characterized using field-emission scanning electron microscopy (FESEM), field-emission transmission electron microscopy (FETEM), X-ray diffraction (XRD) and fluorescence spectrometer. The results showed that the crystalline size of TiO_2 nanopowders was attributed to Y-doping content, it decreased with the increase of Y-doping content, the crystalline size decreased from 15.9nm to about 9.3nm when Y-doping content increased to 2 at.%. While Y doping had little influence on the morphology of TiO_2 nanotubes, pure and Y-doped TiO_2 nanotubes were both about 8 nm in outer diameter and 100-500 nm in length with open ends and hollow structure. Moreover, the crystallinity of TiO_2 nanotubes were generally less than that of TiO_2 nanopowders, the appropriate Y-doping content can keep a certain degree of crystallinity of TiO_2 nanotubes. FS intensities of TiO_2 nanopowders and nanotubes were affected by Y-doping content, FS intensities of TiO_2 nanotubes increased firstly and then decreased with the increase of Y-doping content, FS intensities of TiO_2 nanopowders and nanotubes reached the maximum when Y-doping content were 1 at.%. The variation of photocatalytic properties and FS intensities with the increase of Y-doping content is mostly similar, the photocatalytic properties of TiO_2 nanopowders and nanotubes reached the maximum when the Y-doping content were 0.5 at.% and 1 at.% respectively. Under the same conditions of Y-doping content, TiO_2 nanotubes exhibited a higher photocatalytic activity than TiO_2 nanopowders.

Keywords: Y-doped; TiO2; Nanotube; Photocatalytic; Photoluminescence

1. INTRODUCTION

Semiconductor photocatalysts have extensive application prospect in clean energy, environmental protection, textile industry and medical health [1, 2]. Among numerous semiconductor

photocatalysts, nano-TiO_2 has attracted considerable interest due to its non-toxic, inexpensive, light resistance and stable chemical properties. Nano-TiO_2 is considered to be one of the most promising semiconductor materials [3, 4]. But for the pure nano-TiO_2, the disadvantage of the short lifetime of excited electron–hole pairs reduces the photocatalytic performance and limits its wider application [5]. In order to improve the photocatalytic performance of TiO_2, the modification of TiO_2 becomes hot research topic [6, 7]. Doping is a commonly used method for modification [8], and rare earth elements doping has long been known as one of the most effective method to improve photocatalytic performance [9]. Rare earth doping create more oxygen defects, which can effectively restrain the recombination of photo-generated electron-hole pairs in the transfer process, rare earth doping is also possible to form impurity level, which can improve the effective utilization of photo-induced carriers, these factors are simultaneously contributing to the improvement of photocatalytic performance [10, 11]. Y^{3+} radius (0.089nm) is similar to the Ti^{4+} radius (0.068nm), therefore, Y^{3+}may replace Ti^{4+} and enter into the TiO_2 lattice，which leads to the lattice distortion. In addition, Y energy level is close to TiO_2 conduction band, so Y doping can reduce electron-hole pair recombination rate, thereby improving the photocatalytic properties of nano-TiO_2. Studies have shown that Y doping can improve the photocatalytic activity of TiO_2 nanopowders and nano films [12, 13]. Fluorescence spectroscopy (FS) is an effective method to study the electronic structure and optical properties of nano semiconductor materials, it is possible to obtain the information of optical carriers migration, capture and composite, and surface oxygen defects**.** By studying the photoluminescence performance of photocatalyst can understand the photocatalyst surface defect information, the photocatalyst surface electron-hole pair's capture, and transfer and separation processe [14, 15].

At present, the studies of pure and doped nano-TiO_2 mainly concentrate on the nanopowders, nanorods and nanofilms [16-18]**,** and the study of titanium oxide nanotubes mainly focused on the synthesis, doping modification, photocatalytic properties and applications [19-21], there are few reports on the luminescence properties and the relationship of photocatalytic properties and luminescence properties of nanotubes. In addition, few researches have investigated the effects of doping on the crystallinity of TiO_2 nanotubes too. And we all know, the photocatalytic properties of photocatalysts depend not only on their composition but also on their morphology, phase and crystallinity [22, 23]**.**

Up to now, different nanostructures of pure or doped TiO_2 had been prepared via different methods, such as: TiO_2 nanoparticles prepared by sol–gel method [24]**,** TiO_2 nanofibers or nanorods by electrospinning method, thermal hydrolysis and the subsequent calcination [25], and TiO_2 nanotubes. In contrast of the others nanostructures of TiO_2, nanotube can not only provide higher electron mobility, but also has high specific surface area, these allow it to have excellent photocatalytic activity [26]. There are various methods for fabricating TiO_2 nanotube: template synthesis, hydrothermal synthesis and anodic oxidation methods [27-29]**.** However, these methods are complex and time consuming. By contrast, microwave refluxing is a simple method for synthesizing nano materials. In this method, the energy of microwave radiation can be quickly applied to the materials. Therefore, using this technology can reduce reaction time and cost [30, 31].

In this study, we synthesised pure and Y-doped TiO_2 nanotubes using a microwave refluxing method. Further, using comparative studies, the morphology, crystallinity and the photoluminescence

properties of the synthesised TiO_2 nanotubes and nanopowders were investigated. Finally, the relationship of the photocatalytic properties and the photoluminescence properties were also studied.

2. EXPERIMENTAL

2.1 Materials

The raw materials used in this experiment were all analytical grade and obtained from Chongqing Chuandong Chemical Reagent Co., Ltd., China. Self-made deionized water was used in the whole experiment.

2.2 Synthesis of TiO_2 nanopowders and nanotubes

TiO_2 nanopowders were prepared by sol-gel method with two different solutions called A solution and B solution. A solution contains 20 ml deionized water, 20 ml acetic acid, 80 ml alcohol and different contents $Y(NO_3)_3$, B solution contains 80 ml alcohol mixed with 40 ml butyl titanate, which all were mixed under magnetic stirring respectively. Next, A solution was added to B solution slowly using an acid buret under magnetic stirring, then the uniform mixture was aged for 24 hours and dry in 80°C, and then, was calcined at 500 ℃ in a high temperature resistance furnace (SRJK-4-13, Jiangsu Dongtai Resistance factory), grinded and 400 mesh sieved, finally, TiO_2 nanopowders with 0.0 at.%, 0.5 at.%, 1 at.%, 1.5 at.% and 2 at.% Y doped (n_Y:n_{Ti}) were prepared, and marked as Y0-TiO_2, Y0.5-TiO_2, Y1-TiO_2, Y1.5-TiO_2 and Y2-TiO_2, respectively.

0.2 g of the as-prepared TiO_2 nanopowders were added to 50 ml NaOH aqueous solution (10 mol/L) and stirred using an ultrasonic dispersion instrument for 10 min. Then, the mixture was transferred to a Teflon flask (150 ml), which was put in a microwave refluxing reactor (LWMC-205, Shanghai Qing Apple Instrument Co., Ltd.). The microwave power was set to 500 W, and the reaction time was 90 min. The product was washed and separated by centrifuge repeatedly until the pH was reached to 7. After dried at 80 °C, the pure and Y-doped TiO_2 nanotubes were synthesized, the as-prepared samples were marked according to the different Y-doping contents: Y0-TiO_2NT， Y0.5-TiO_2NT， Y1-TiO_2NT，Y1.5-TiO_2NT and Y2-TiO_2NT respectively.

2.3 Characterisation of crystalline structure

The crystalline structures of TiO_2 nanotubes and nanopowders were characterized by X-ray diffraction (XRD, D/MAX-2500PC, λ=0.15418nm, Japan) with Cu Kα radiation in the two theta degree ranging from 10° to 90°. The morphologies of the as-prepared samples were observed with a field emission scanning electron microscope (FESEM, NOVA400, America) and a field emission transmission electron microscopy (FETEM, LIBRA200, Germany). All samples were put into a beaker filled with deionized water and dispersed using an ultrasonic dispersion instrument for 10 min before FESEM and FETEM sampling.

2.4 Characterisation of photoluminescence

The characterisation of photoluminescence of TiO_2 nanotubes and nanopowders were determined by FS spectra (Shimadzu RF-5301PC, Japan), the excitation wavelength (λ_{ex}) was set at 350nm.

2.5 Characterisation of photocatalytic activity

The photocatalytic activities of the samples (include nanopowders and nanotubes) were determined by adding the samples to the methyl orange solution as the catalyst to test the degradation rate of methyl orange. Since the degradation rate of methyl orange is proportional to the absorbance, so that the degradation rate can be calculated using the formula: $\eta = (C_0-C_t)/C_0 \times 100\%$, where C_0 and C_t are the absorbances at 0 min and t min, respectively.

During the measurements, 20mg samples were added to 10 ml methyl orange solution (10 mg/L). Then the mixture was dispersed with ultrasonic instrument for 10 min. Then this mixture was put in a homemade photocatalytic device. In the device, multiple quartz glass tubes containing the mixture were put around an ultraviolet lamp at an equal distance of 15 cm. The power of the ultraviolet lamp was 15 W. After each set time, the samples and methyl orange mixtures were separated by centrifugation. The absorbance of the methyl orange solution after the degradation was investigated by a 722N spectrophotometer (Shanghai Precision Scientific Instrument Co., Ltd.). The mixture was dispersed again with ultrasonic instrument before each photocatalytic experiment. Tests showed that in the absence of light irradiation and with no samples in the methyl orange solution, the absorbance of methyl orange solution did not change significantly.

3. RESULTS AND DISCUSSION

3.1 Morphology

The SEM morphology of pure and Y-doped TiO_2 nanotubes prepared by a microwave refluxing method using Y $(NO_3)_3$ as doping source are shown in Fig. 1. The TEM morphology of pure and Y-doped TiO_2 nanopowders and nanotubes are shown in Fig. 2.

As it can be seen from Fig. 1 and Fig. 2 (d, e, f), TiO_2 nanotubes had uniform size with open ends and hollow structure, the outer diameters are both about 8 nm, the inner diameters are about 5 nm ， the lengths are 100-500 nm, Y doping had little influence on the morphology of TiO_2 nanotubes when Y-doping content is 0 at.% to 2 at.% in this study.

Fig.2 (a, b, c) shows the TEM morphology of pure and Y-doped TiO_2 nanopowders prepared by sol-gel method and subsequently calcined at 500 ℃, it can be seen that the crystalline size of nanopowders is about 9-20 nm. The crystalline size of pure TiO_2 nanopowders is about 20 nm with a little agglomeration. With the increase of Y-doping content, the crystalline size decreased, the agglomeration is gradually serious; when Y-doping content increased to 2 at.%, the crystalline size of nanopowders is reduced to about 9nm, and the agglomeration became more serious. This is mainly

because: on the one hand, in the sol-gel process, the precursor of titanate reacted with NO^{3-} and obtained $TiO(NO_3)_2$ when doped source Y $(NO_3)_3$ was added in. Meanwhile, NO^{3-} can also acts as the action of a chelating agent [32], both of which can slow down the condensation reaction rate, thereby controlling the nucleation and growth process. On the other hand, Y elements can strongly inhibit the conversion of TiO_2 crystal phase, thus improve the temperatures of phase transformation of TiO_2 from anatase to rutile [33], and hindered the TiO_2 crystalline growth during calcination.

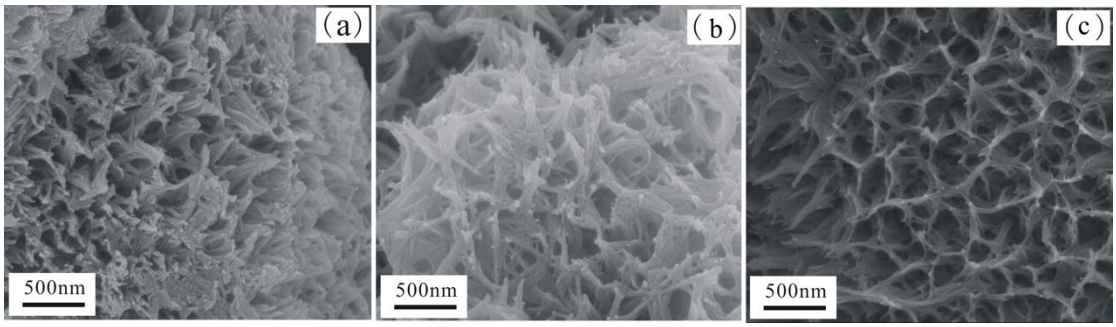

Figure 1. SEM images of TiO_2 nanotubes (a)Y0-TiO_2NT，(b)Y1-TiO_2NT，(c)Y2-TiO_2NT

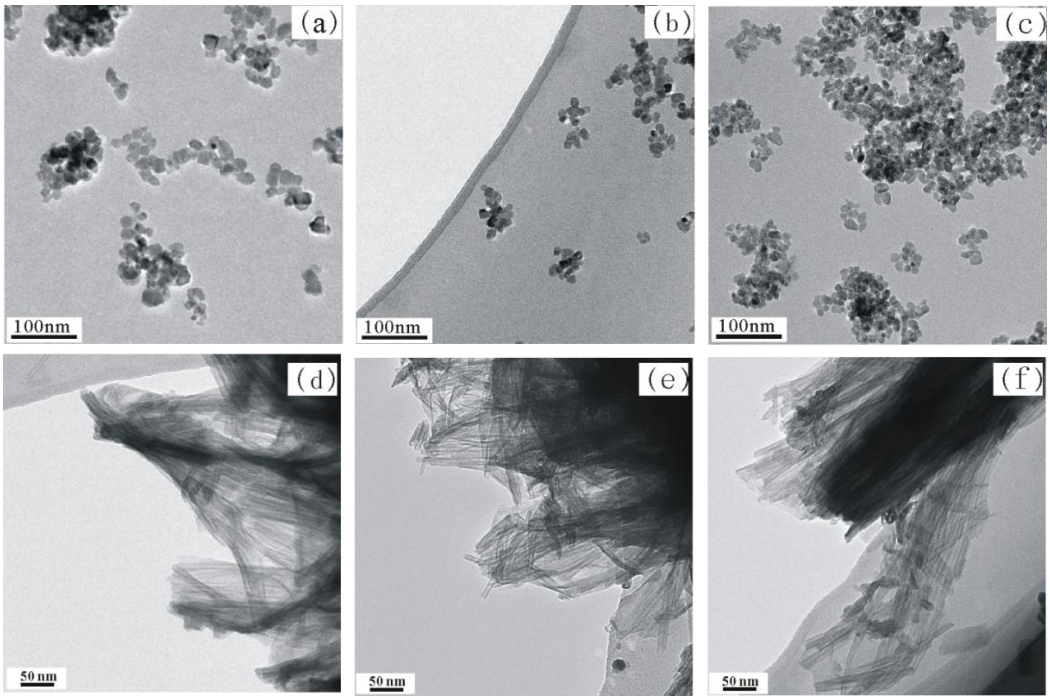

Figure 2. TEM images of TiO_2 (a) Y0-TiO_2; (b) Y1-TiO_2; (c) Y2-TiO_2; (d) Y0-TiO_2NT; (e) Y1-TiO_2NT; (f) Y2-TiO_2NT

3.2 Crystal form

The phases of the synthesised nanopowders and nanotubes were identified through XRD measurements. Fig. 3 shows the XRD patterns of the pure and Y-doped TiO_2 nanopowders and

nanotubes. The average crystalline size of the nanopowders was calculated using Debye-Sherrer formula [34] :

$D=0.89\lambda/\beta\cos\theta$

Where D is the crystalline size of nanopowders (nm), λ is X-ray wavelength (λ=1.541874 A), β is full width at half-maximum (FWHM) of the characteristic peaks and θ is the Bragg diffraction angle. The crystallinity of samples was calculated by software MDI jade 5.0 according to the characteristic peaks of XRD patterns. Table 1 shows the calculated average crystalline size and crystallinity of the nanopowders. It can be seen in Table 1 that the crystalline size of the nanapowders decreased evidently with the increase of Y-doping content, when Y-doping content increased to 2 at.%, the crystalline size of TiO_2 nanopowders decreased to about 9.3nm, this calculation results are in agreement with the TEM results basically.

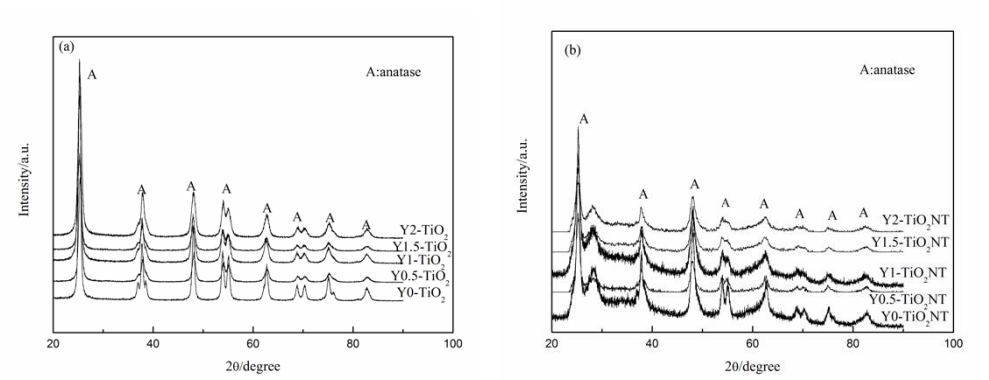

Figure 3. XRD patterns of TiO_2(a) Pure and Y-doped TiO_2 nanopowders; (b) Pure and Y-doped TiO_2 nanotubes

XRD patterns of TiO_2 nanopowders and nanotubes (see Fig. 3) showed the obvious characteristic peaks of the anatase phase (JCPDS Card No.21-1272) , and the characteristic peaks of Y_2O_3 were not found in the XRD patterns (Y_2O_3: JCPDS Card No. 86-1326). This is because that some Ti^{4+} had been replaced by Y^{3+} and Y^{3+} enter into TiO_2 lattice [12], or Y_2O_3 content was too small to be detected, the samples were essentially anatase TiO_2.

XRD patterns of pure and Y-doped TiO_2 nanopowders (see Fig. 3(a)) shows that the characteristic peaks appear different degree wider and the intensity of diffraction peaks decreased with the increase of Y-doping content. Analysis suggests that Y^{3+} radius is similar to the Ti^{4+} radius, Y^{3+} can enter into the TiO_2 lattice and replace part of Ti^{4+} [13], cause lattice distortion, formed microstress, resulting in a lower crystallinity (see Table.1) and lower diffraction intensity, and wider diffraction peak. Compared of nanotubes with the corresponding nanopowders, it can be found that the diffraction peaks intensity decreased and the width increased, suggest that the lattice distorted and the crystallinity decreased [35]. This is because that TiO_2 nanocrystalline was stripped into nanosheet in NaOH solution in the process of TiO_2 nanotube preparation [36], and caused the crystal lattice changed, resulting in lower crystallinity. In addition, compared with the other nanotubes, sample Y0.5-TiO_2NT had the slightly higher characteristic peak intensity and crystallinity (see Fig. 3(b) and Table 1). This

indicates that the appropriate Y-doping content can maintain the crystallinity of TiO_2 nanotubes，the reason needs further study.

Table 1. Physicochemical properties of TiO_2.

TiO_2	The contents of Y(at.%)	Crystalline size(nm)	Crystallinity (%)
nanopowders	0%	15.9nm	96.03%
	0.5%	13.1nm	90.83%
	1%	12.3nm	88.04%
	1.5%	11.2nm	85.53%
	2%	9.3nm	82.90%
Nanotubes	0%	-	71.16%
	0.5%	-	83.40%
	1%	-	72.66%
	1.5%	-	72.39%
	2%	-	71.97%

3.3 Photoluminescence properties

Fig. 4 shows the fluorescence spectra (FS) of pure and Y-doped TiO_2 nanopowders, and Fig. 5 shows the FS of pure and Y-doped TiO_2 nanotubes.

The results showed that when excitation wavelength (λ_{ex}) was set at 350nm, all samples exhibited strong and broad emitting signal within the visible range 400-600nm, and FS peak appeared at 450nm, 468nm and 482nm; 450nm and 468nm belong to the free exciton luminescence, and 482nm belongs to bound exciton luminescence. FS of all samples have similar shapes, FS peaks exhibited consistent and Y doping did not form new FS feature peaks, but the peaks height had changed. This suggested that Y doping did not cause new FS phenomenon, but it made the FS intensity changed.

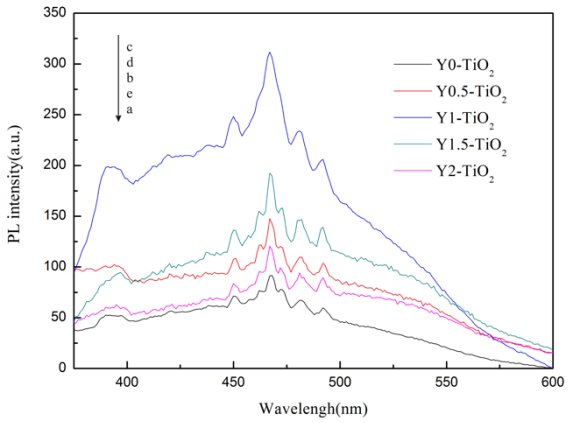

Figure 4. FS of TiO_2 nanopowders (a)Y0-TiO_2; (b)Y0.5-TiO_2; (c)Y1-TiO_2; (d)Y1.5-TiO_2; (e)Y2-TiO_2

FS peak of TiO_2 nanopowders and nanotubes firstly increased and then decreased with the increase of Y-doping content. FS peak of TiO_2 nanopowders and nanotubes reached the maximum when Y-doping content reached 1 at.%. FS intensity of nanotubes is higher than those of nanopowders with the same Y-doping content, it increase about 25%.

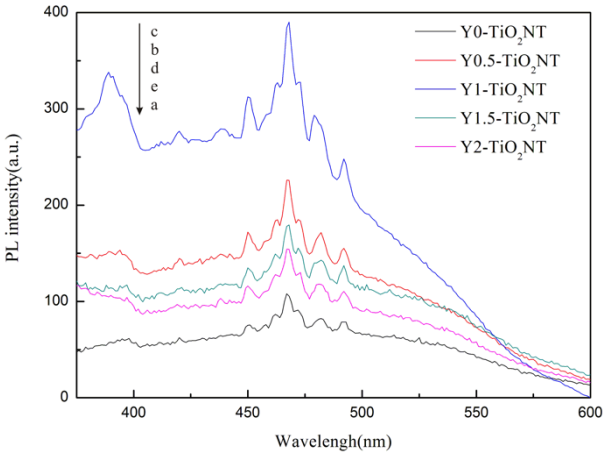

Figure 5. FS of TiO_2 nanotube (a) Y0-TiO_2NT; (b)Y0.5-TiO_2NT; (c)Y1-TiO_2NT; (d)Y1.5-TiO_2NT; (e)Y2-TiO_2NT

3.4 Photocatalytic property

Fig. 6 shows the relationship of C_t/C_0 and *t.* It can be seen from the diagram that Y doping can improve the photocatalytic properties of TiO_2 nanopowders and nanotubes.

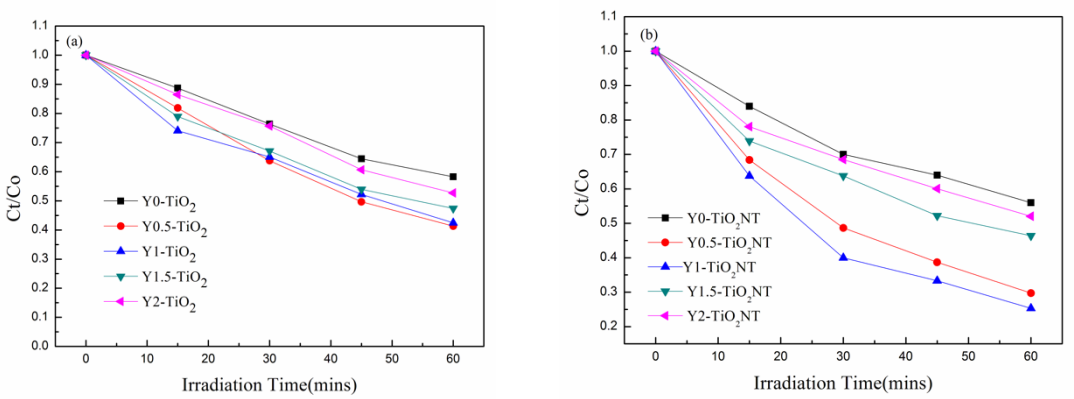

Figure 6. TiO_2 degradation of methyl orange (a) the pure and Y-doped TiO_2 nanopowders; (b) Pure and Y-doped TiO_2 nanotubes

Fig.6 (a) shows the degradation rate of methyl orange when the nanotubes were used as a photocatalyst. It can be seen that the photocatalytic properties firstly increased and then decreased with the increase of Y-doping content, the photocatalytic properties of TiO_2 nanopowders reached the

maximum when Y-doping content was 0.5 at.%. The main reason is: On the one hand, Y doping led to the crystalline size of TiO_2 nanopowders decrease and the lattice distort, so that the oxygen vacancies and defect concentration increased, resulting in more electron-hole capture traps [37], reduced the electron-hole pair recombination rate, thereby improving photocatalytic efficiency. On the other hand, Y doping can introduce impurity levels for TiO_2 [38], resulting in the narrowing of TiO_2 band gap and the red shift of absorption bands, this can stimulate more electronic transitions, thus improve the photocatalytic properties. But the photocatalytic properties of TiO_2 nanopowders became lower, with the Y doping further increase. The reason is: the band gap of TiO_2 became narrower because of the overmuch Y doping, on the contrary, improve the electron-hole pair recombination rate, thereby reduced its photocatalytic properties.

Fig.6 (b) shows the degradation rate of methyl orange when the nanotubes were used as a photocatalyst. The photocatalytic properties firstly increased and then decreased with the increase of Y-doping content, the photocatalytic properties of TiO_2 nanotubes reached the maximum when Y-doping content was 1 at.%, the reason is similar to those of nanopowders, it mainly due to the lattice distortion and band gap narrowing. And in the same Y-doping content condition, TiO_2 nanotubes exhibited a higher photocatalytic activity than TiO_2 nanopowders, this is because that TiO_2 nanotubes with tubular structure had more specific surface area than TiO_2 nanopowders, and increased the photocatalytic reaction area, to further improve the photocatalytic properties.

4. CONCLUSIONS

In summary, Y-doped anatase TiO_2 nanotubes were fabricated by a microwave refluxing method using self-made Y-doped anatase TiO_2 nanopowders as precursor. The method is a fast and easy one and does not require a template or the subsequent calcination. The crystalline size of precursor TiO_2 nanopowders prepared by sol–gel method, the crystallinity of nanopowders and nanotubes, the FS intensity of TiO_2 nanotubes and nanopowders, and the photocatalytic property of TiO_2 nanopowders and nanotubes were all affected by Y-doping content, except for the morphologies of nanotubes.

The crystalline size of TiO_2 nanopowders decreased with the increase of Y-doping content, the crystalline size decreased to about 9.3nm when Y-doping content increased to 2 at.%. The crystallinities of nanopowders decreased with the increase of Y-doping content, but the appropriate Y-doping content can keep a certain degree of crystallinity of TiO_2 nanotubes. FS intensities of TiO_2 nanotubes firstly increased and then decreased with the increase of Y-doping content, FS intensity of TiO_2 nanopowders and nanotubes reached the maximum when Y-doping content were 1 at.%. The photocatalytic properties increased with the increase of Y-doping content; the photocatalytic properties of TiO_2 nanopowders and nanotubes reached the maximum when Y-doping content were 0.5 at.% and 1 at.% respectively. Under the same conditions of Y-doping content, TiO_2 nanotubes exhibited a higher photocatalytic activity than TiO_2 nanopowders. Compared with the pure nanotubes, the photocatalytic activity of Y-doped one increased by 27.7%. There is a certain relationship between the photocatalytic activity and the FS intensity of nanopowders and nanotubes, that is, the variation of

photocatalytic properties and FS intensity with the increase of Y-doping content is mostly similar, but when they reach the maximum value, the corresponding Y-doping content is different, the reason needs further study.

ACKNOWLEDGEMENTS
This work was supported by the Fundamental Research Funds for the Central Universities (Project No.CDJZR12130044) and Sharing Fund of Chongqing University's Large-scale Equipment No.201506150002)

References

1. L. L. Xu, Z. L. Wang, H.L. Song and L. J. Chou, *Catal. Commun.*, 35 (2013) 75.
2. T. Thongkanluang, T. Kittiauchawal and P. Limsuwan, *Ceram Int.*, 37 (2011) 543.
3. E. L. Boulbar, E. Millon and C. B. Leborgne, *Thin Solid Films*., 553 (2014) 13.
4. S. Maja and A. Biljana, *J Sol-Gel Sci Techn*., 61(2012) 390.
5. Z. Hamden, D.P. Ferreira, L.F. Vieira Ferreira and S. Bouattour, *Ceram Int.*, 40(2014) 3227.
6. S. Karapati, T. Giannakopoulou, N. Todorova, N. Boukos, D. Dimotikali and C. Trapalis, *Appl Catal B-Environ*., 176 (2015) 578.
7. W. P. Chen, A. H. Zhou, X. Yang and Y. Liu, *J Alloy Compd.*, 210 (2014) 138.
8. I. R. Vázquez, G. D. Angel, V. Bertin, F. González, A. V. Zaval, A. Arrieta, J. M. Padilla, A. Barrera and E. Ramos-Ramirez, *J Alloy Compd.*, 643 (2015) S144.
9. E. L. Boulbara, E. Millon, C. B. Leborgne, C. Cachoncinlle, B. Hakim and E. Ntsoenzok, *Thin Solid Films.*, 553 (2014) 13.
10. F. W. Wang, M. Xu, L. Wei, Y. J. Wei, Y. H. Hu, W. Y. Fang and C. G. Zhu, *Electrochim Acta*, 153 (2015) 170.
11. Y. T. Ma and S. D. Li, *J Chin Chem Soc-Taip.*, 62 (2015) 380.
12. M. Khan and W. B. Cao, *J Mol Catal A-Chem.*, 376 (2013) 71.
13. W. J. Zhang, K. L. Wang, S. L. Zhu, Y. Li, F. H. Wang and H. B. He, *Chem Eng J.*, 155 (2009) 83
14. A. Bhogale, N. Patel, P. Sarpotdar, J. Mariam, P. M. Dongre, A. Miotello and D.C. Kothari, *J Mol Catal A-Chem*., 102 (2013) 257.
15. G. Carturan, R. D. Maggio, M. Montagna, O. Pilla and P. Scardi, *J Mater Sci.*, 25 (1990) 2705.
16. N. N. Ilkhechi, B. K. Kaleji, E. Salahi and N. Hosseinabadi, *J Sol-Gel Sci Techn.*, 74 (2015) 765.
17. Z. W. Yang, B. Wang, H. Cui, H. An, Y. Pan and J. P. Zhai, *J Phys Chem C*., 119 (2015) 16905.
18. W. G. Zhang, Y. M. Liu, D. Y. Zhou, J. Wen, W. Liang and F. Q. Yang, *Rsc Adv*., 5 (2015) 57155
19. Y. Yu, X. J. Yu and S. L. Yang, *J Mater Sci-Mater El*., 26 (2015) 5715
20. M. M. Momeni, Y. Ghayeb and Z. Ghonchegi, *Ceram Int*., 41 (2015) 8735
21. J. P. Carroll, E. Panaitescu, B. Quilty, L. L. Wang, L. Menon and S. C. Pillai, *Appl Catal B-Environ.*, 176 (2015) 70
22. J. J. Wu1, X. J. Lü, L. L. Zhang, F. Q. Huang and F. F. Xu, *Eur J Inorg Chem*., 19 (2009) 2789
23. J. N. Ding, Y. Li, H. W. Hu, L. Bai, S. Zhang and N. Y. Yuan, *Nanoscale Res Lett*., 8 (2013) 1
24. H. Eskandarloo, A. Badiei, M. A. Behnajady and G. M. Ziarani, *Ultrason Sonochem*., 26 (2015) 281.
25. D. S. Yao, Y. L. Zhao, L. Zhu, J. Song, X. Q. Gu, J. J. Zhu and Y. H. Qiang, *Int. J. Electrochem. Sci*., 10 (2015) 5914.
26. D. Fang, Z. P. Luo, K. L. Huang and D. C. Lagoudas, *Appl Surf Sci.*, 210 (2014) 138.

27. H. Zhao, K. Y. Zheng, Y. Sheng, H. B. Li, H. G. Zhang, X. F. Qi, Z. Shi and H. F. Zou, *J Solid State Chem.*, 210 (2014) 138.
28. D. Aphairaj, T. Wirunmongkol, S. Niyomwas, S. Pavasupree and P. Limsuwan, *Ceram Int*., 40 (2014) 9241.
29. H. Song, J. Shang and C. Suo, *J Mater Sci Technol.*, 31 (2015) 23.
30. J. Giri, T. Sriharsha and D. Bahadur, *J. Mater. Chem.*, 14 (2004) 875.
31. J. L. Su, H. S. Xue, M. Gu, H. Xia and F. S. Pan, *Ceram. Int.*, 40(2014) 15051.
32. M. Crisan, R. Malina, N. Dragan and D. Crisan, *Appl Catal A-Gen.*, 504 (2015) 130.
33. K.S.Kumar, C. G. Song, G. M. Bak, G. Heo, M. J. Seong and J. W. Yoon, *J Alloy Compd*., 617 (2014) 683.
34. T. Adinaveen, J. J. Vijaya and L. J. Kennedy, *J Supercond Nov Magn.*, 27 (2014) 1721.
35. J. D. Fidelus, Y. Zhydachevskii, W. Paszkowicz, A. Reszka, P. Dluzewski and A. Suchocki, *Opt Mater*., 47 (2015) 361.
36. J. Yu, H. Yu, B. Cheng, C. Trapalis, *J. Mol. Catal. A: Chem.*, 249 (2006) 135. 004.
37. C. D. Valentin, G. Pacchioni, H. Onishi and A. Kudo, *Chem. Phys. Lett.*, 469 (2009) 166.
38. X. Niu, S. Li, H. Chu and J. Zhou, *J. Rare Earths*., 29 (2011) 225.